Determination of the Forming Limit Diagrams Using Image Analysis by the Corelation Method

P. Vacher, A. Haddad, R. Arrieux (2)
Laboratoire de Méchanique Appliquée, Ecole Supérieure d'Ingénieurs d'Annecy,
Université de Savoie, Annecy, France
Received on January 8, 1999

Abstract

This paper deals with a new method of strain measurement applied to the experimental determination of the forming limit diagrams of thin steel sheets. This method uses the correlation technique to determine the displacement field between two images taken on the same area of the sample at two different strain levels. The strains are calculated from this field. The range of strains determined between two images may be very wide. This allows to compare the initial image to one before the sample fracture or two successive images during the straining. This method shows that the strain localization may occur early during the forming process and so the onset of localized necking is not a sudden phenomenon. A method is proposed to draw the forming limit diagrams for necking.

Keywords : Strain measurement, Image analysis, Forming limit diagrams.

1 INTRODUCTION

The numerical simulation of deep drawing operations needs efficient tools to predict the onset of localized necking. Nowadays engineers have at their diposal very efficient FEM calculation software to simulate the material flow during a forming operation, but these tools generaly can't predict its feasibility if they have not integrated a necking criterion.
The first criterion proposed is the classical forming limit diagram. It is generally determined by experiment and can only be used for the prediction of necking for single stage formed parts because it strongly depends on the strain path shape. A second criterion is the forming limit stress diagram, it is independant of the strain path shape and so it can predict the necking occurrence for single and for several stage forming. It is generally determined by means of a step by step plastic calculation along experimental strain paths. So both criteria need very accurate strain measurements and a precise detection of the instant when the necking occurs.
Untill now the strain determination was done using grid patterns laid on the sheet surface using chemical coatings. The deformations were determined by optical measurement of the grid distorsions. This method has been automatized but its accuracy is rather low. Another problem is the detection of the onset of necking. Classicaly this operation is carried out from fractured samples and many methods were proposed to estimate the strains values at the onset of necking. Of course, they lack of accuracy because it is difficult to determine the necking occurrence from a brocken part .
In this study we propose a method of strain measurement using a random grey level surface and of necking detection by analysing of the numerical images of the sample straining.

2 STRAIN MEASUREMENT METHOD.

2.1 Displacement field determination

The principle of this method is to compare two digital images of the sample surface first painted in a random way. The first one recorded before straining, and the second one after or during the forming operation. Some precautions must be taken in the random grey level surface preparation :
- mat spray paints to avoid any reflections,
- the average spot size must be lower than 20 pixels,
- the grey levels can vary between 0 and 255 but must evolve steadily between two neighbouring pixels.

To analyse large strains (>60%), it is necessary to carry out the forming of the sample a short time after the paint application on the sample (>1h), otherwise the coating will dry up and may not resist to the large straining.
These images will be compared using a grey level correlation coefficient in order to find the initial image points on the final image with a precision lower than the camera pixel. For this purpose, the image in which the

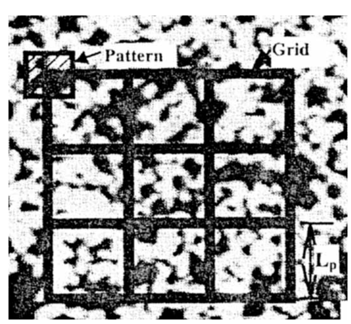

Figure 1 : Definition of the grid element and of correlation pattern

deformations are to be analysed is numerically divided in square grid elements of side Lp pixels, the displacement field will be calculated for each of these square grid elements (figure1). Around each of the four points of one

grid element, a square analysis zone with variable dimensions is used, centered on each of the considered points and called correlation pattern. The principle of this method is to find every points of the grid on the final image by comparison of the grey level.
The initial image grey level is repesented by the discrete function f(x,y) which becomes f*(x*,y*) on the deformed image :

$$f^*(x^*,y^*) = f^* (x+u(x,y), y+v(x,y)) \quad (1)$$

with u(x,y) and v(x,y) the displacement fields for one given grid element. These displacement fields will be obtained by using the correlation between an initial image grid element and its corresponding one in the deformed image. A point of the initial image moves, after straining, to a sub-pixel position. The grey levels on the deformed image are obtained with bilinear or bi-cubic interpolations.

The correlation coefficient used to compare two zones is [1]

$$Cor = 1 - \frac{\int_{\Delta S} f(x,y).f^*(x^*,y^*).dx.dy}{\sqrt{\int_{\Delta S} f(x,y)^2.dx.dy.\int_{\Delta S} f^*(x^*,y^*)^2.dx.dy}} \quad (2)$$

ΔS : area of the concerned correlation pattern on the initial image.
For perfect correlation, f(x,y)=f*(x*,y*), => Cor = 0
For imperfect correlation 0 > Cor > 1
The correlation parameter chosen here is independent of a global modification of the grey levels between the two pictures. It is used as an indicator of the similarity degree between two patterns on initial and final image.
The displacement field, assumed to be bi-linear, has the following form :

$$u_x(x,y) = (du_B - du_A)(x - x_A)/L_p + (du_D - du_A)(y - y_A)/L_p + (du_C - du_B + du_A - du_B)(x - x_A)(y - y_A)/L_p^2 + du_A \quad (3)$$

$$u_y(x,y) = (dv_B - dv_A)(x - x_A)/L_p + (dv_D - dv_A)(y - y_A)/L_p + (dv_C - dv_B + dv_A - dv_B)(x - x_A)(y - y_A)/L_p^2 + dv_A$$

An iterative procedure is used in order to determine the strain field [2]. An initial solution for one point is given apprimately on the final image, then at the first step, this initial solution is applied on the patterns around each grid elements points A,B,C,D. The pattern around point A is translated on the final image. The found point A_0^* is not the solution, and then the pattern is deformed in order to minimise the correlation parameter (figure 2). The gradient method is used for this last operation. These operations are carried out for the other points B C D of the square and for every squares of the grid. So the displacement field is determided in every point of the final image.

2.2 Strain field determination.

The Green-Lagrange's tensor **E** is calculated :

$$\mathbf{E} = 1/2\{\mathbf{F}^T \otimes \mathbf{F} - \mathbf{1}\} \quad (4)$$

where **F** is the gradient transformation tensor.

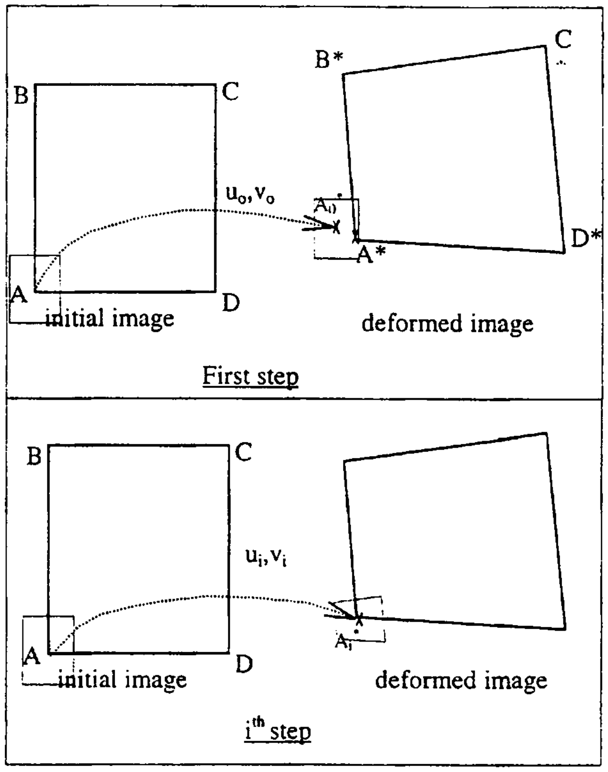

Figure 2 Iterative process for the displacement field determination

In a condensed form, this tensor is written as a function of the displacement :

$$E_{ij} = \frac{1}{2}\{u_{i,j} + u_{j,i}\} + \frac{1}{2} u_{i,k}u_{j,k} \quad (5)$$

with i,j,k ∈ (x,y), and $u_{i,j} = du_i/du_j$

Green-Lagrange's strain tensor values expressed in the principal axes OX and OY are :

$$E_X = \frac{E_{xx} + E_{yy}}{2} + \frac{1}{2}\sqrt{(E_{xx} - E_{yy})^2 + 4.E_{xy}^2} \quad (6)$$

$$E_Y = \frac{E_{xx} + E_{yy}}{2} - \frac{1}{2}\sqrt{(E_{xx} - E_{yy})^2 + 4.E_{xy}^2}$$

The angle between x and X is defined as :

$$\theta = \mathrm{Arctg}\left(\frac{2 * E_{xy}}{E_{xx} - E_{yy}}\right) \quad (7)$$

Generally the strains used for deep drawing operations are expressed using logarithmic strains. These values are calculated in the OXY reference as function of E_X and E_Y.

$$E_{LX} = \frac{1}{2}\ln(2E_X + 1) \quad (8)$$

$$E_{LY} = \frac{1}{2}\ln(2E_Y + 1)$$

So the strains are determined for every points of the studied surface of the sampes.

3 EXPERIMENTAL PROCEDURE

The samples are strained up to fracture by a hydraulic press using the pressure or the displacement rate mode. This press is equiped with a Marciniak's device composed

of a flat headed cylindrical punch (diameter 100mm) a circular die an blank-holder [3]. This method allows to reach every points of the FLD by using blanks with various widths (50mm, 60mm ... 200mm) [4].
The blanks surface are painted in a random way using a black spray of paint, and the pictures are recorded using a CDD camera directly put down on the sample surface in order to keep constant the distance between the camera and the surface. The analysed surface is a square of about 40x40mm. The initial image before the begining of the straining is recorded, the image acquisition system records the last twenty images at the fequency of four images per second. The last image is the one at fracture. The comparison of every image to the initial one don't indicate clearly the image corresponding to the onset of necking [5].Because early during the straining operations, the strains are not homogeneous on the samples surface and we propose here a strain velocity analysis by comparing the successive images of the deformation process. Three kinds of strain paths are be analysed here: uniaxial tension, wide tension and equibiaxial stretching. The studied material is a steel for deep drawing SOLDUR 340 of thickness 1mm.

3.1 Uniaxial tension.

For this test, the straining was stopped when a groove corresponding to the necking was visible on the sample surface. The corresponding image was the number 19. Every image is compared to the previous one in order to determine the strain increment or the strain velocity between two images. On the following images we have plotted the strain value z of every point of the sample surface x y. In Figure 3 corresponding to the strain velocity $d\varepsilon y$, y is the longitudinal axis of the sample between images 14 and 15, we observe that the increments are more important in the center of the analysed area, but every points are more or less strained. The figure 4 corresponds to images 15 and 16, a beginning of strain localization can be seen on a rather wide area of the studied zone. But almost every points have positive strains. On the figure 5 corresponding to images 16 and 17, the strains are located in two narrow secant stripes. Many points of the studied area have no deformation, so we consider that the necking has already appeared on image 17. The observation of the figure 6 confirms the strain localization in a narrow area of the surface, with no deformation elsewhere. So we consider that the image corresponding to the onset of localized necking is the n° 16, because this is the last image where the strain velocity is different from 0 in every points. Now to determine the strain value at the onset of necking we compare this image with the initial one before straining. The strain value at the onset of necking is the average of the 100 higher values of the considered image.

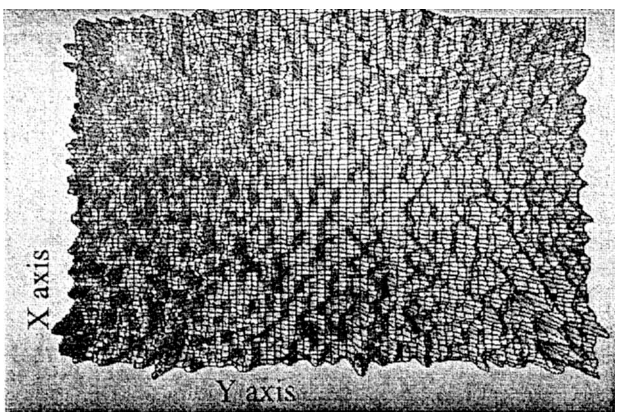

Figure 3 Strain velocity map between images 14 and 15

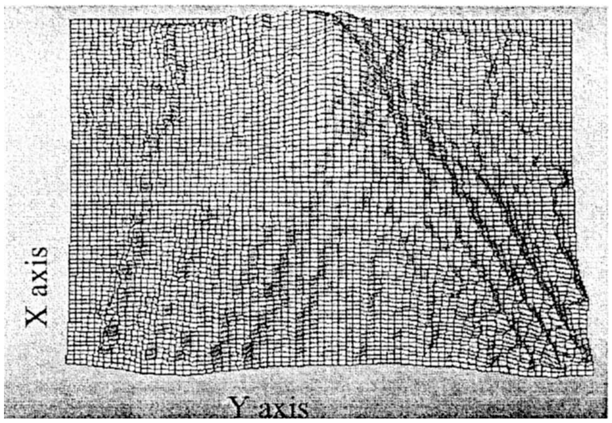

Figure 4 Strain velocity map between images 15 and 16

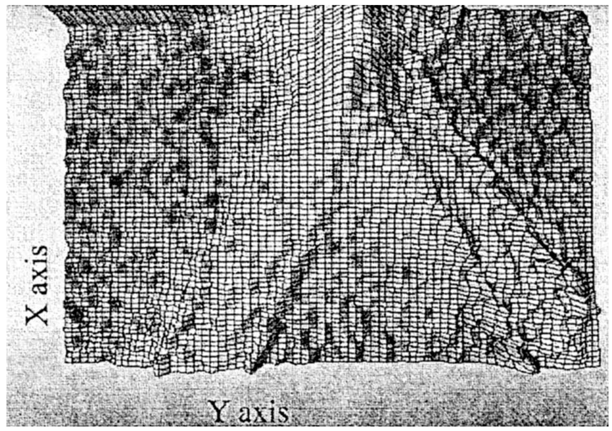

Figure 5 Strain velocity map between images 16 and 17

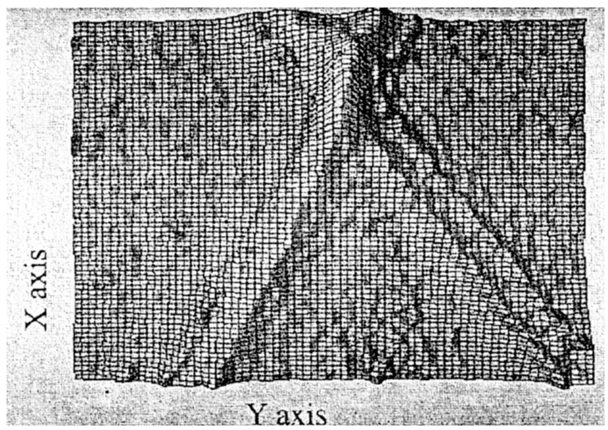

Figure 6 Strain velocity map between images 17 and 18

3.2 Wide tension.

Here no necking was visible before fracture, so the last image (n°20) is the one at fracture. In the first time, every image is compared to the previous one
For this sample (width 120mm), according to the punch and the die diameters (respectively 90 and 110 mm) most of the strains are located in the central part of the sample surface and very early the strains are heterogeneous.. On figure 7, corresponding to images 9 and 10 , the strains are more or less uniformly located on the analysed area, nevertheless they seem to be a little bit higher in a central strip paralell to the horizontal axis, while on figure 8 (images 10 11) we observe a neck which is confirmed on the following image. So image 10 is selected.

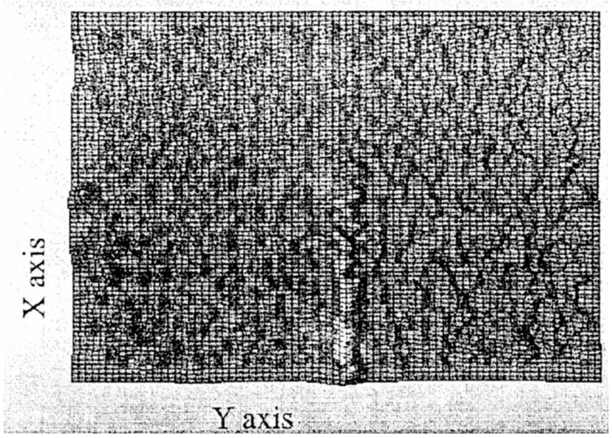

Figure 7 Strain velocity map between images 9 and 10

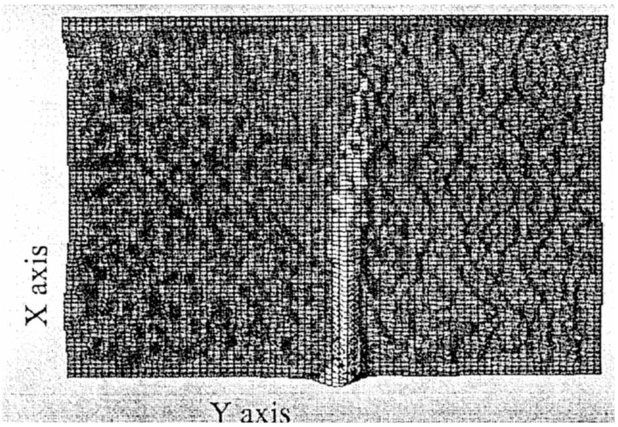

Figure 8 Strain velocity map between images 10 and 11

3.3 Biaxial stretching.

This circular sample was strained up to fracture. On its surface, parallel stripes of localization can be observed. The same procedure of image analysis allows to observe that the onset of necking occurs on image n°17 (Figure 10), while on Figure 11 the strain localization is very clear mainly in one stripe but other ones develop.

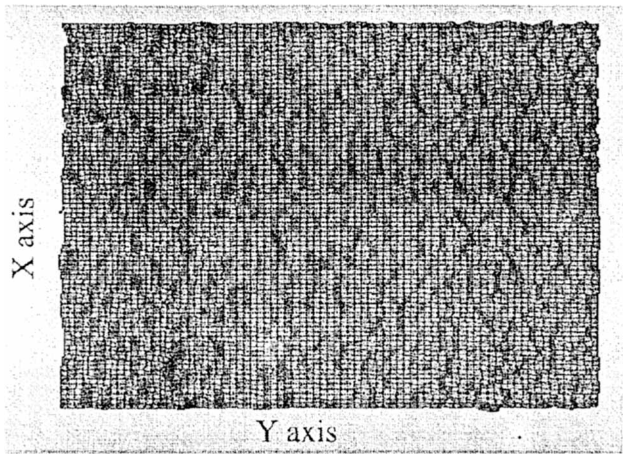

Figure 10 Strain velocity map between images 16 and 17

3.4 Forming limit diagram.

When the picture corresponding to the onset of necking is selected, the software calculates the strains along x and y direction. This method allows to plot the forming limit diagram of the studied material (figure 12).

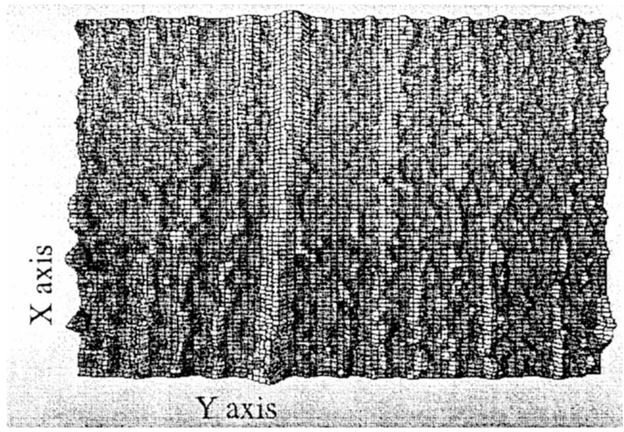

Figure 11 Strain velocity map between images 17 and 18

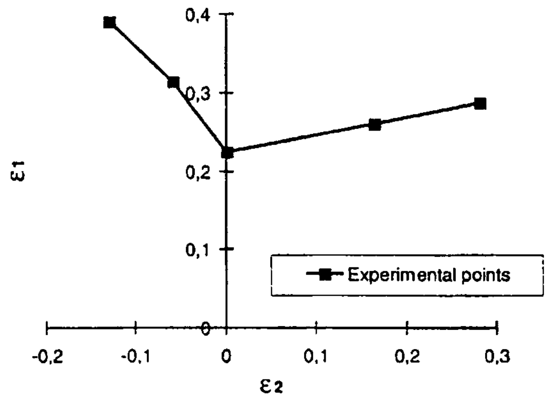

Figure 12 Forming limit diagram.

4 CONCLUSIONS

This method allows to estimate the instant of the necking occurence by analysing the strain increments between the successive images of the straining operation.
We consider that the localization has occured when the strains are located only in a zone of the image, and they are zero elsewhere. Then the comparison of the corresponding image to the initial one allows to calculate the strains ϵ_1 and ϵ_2 at the onset of localized necking and to plot the forming limit diagrams. It gives also very good data for the forming limit stress diagram calculation.

[1] Kahn-Jetter, Z.L., Jha, N.K, Bathia H., 1994 Optimal image correlation in experimental mechanics, Optical Engineering. 33/4 : 1099-1105

[2] Mguil-Touchal,S. Morestin,F. Brunet,M., 1997 Various experimental application of digital image correlation method, Proc. Computer Method and Experimental measurement 97, Rhodes, 21/5 23/5 : 46-58

[3] Gronostajski,J., Dolny, A., 1980 Determination of the forming limit curves by means of Marciniak's punch. Mem. Sci. Rev. Metal. 4 : 570-578.

[4] Arrieux,R., Chalons, J.M., Bedrin,C. Boivin,M., 1984 Computer aided method for the determination of the FLD at necking, Annals of the CIRP 33/1,171-174

[5] Vacher, P., Dumoulin,S. Morestin,F., Mguil-Touchal,S., Bidimensional strain measurement using digital image. Journal of Mech. Eng. Mat. Sciences. (to be published)